



# Observation of Global Hyperon Polarization in Ultrarelativistic Heavy-Ion Collisions

Isaac Upsal for the STAR Collaboration<sup>1</sup>

Ohio State University, 191 W. Woodruff Ave., Columbus, OH 43210

## Abstract

Collisions between heavy nuclei at ultra-relativistic energies form a color-deconfined state of matter known as the quark-gluon plasma. This state is well described by hydrodynamics, and non-central collisions are expected to produce a fluid characterized by strong vorticity in the presence of strong external magnetic fields. The STAR Collaboration at Brookhaven National Laboratory's Relativistic Heavy Ion Collider (RHIC) has measured collisions between gold nuclei at center of mass energies  $\sqrt{s_{NN}} = 7.7 - 200$  GeV. We report the first observation of globally polarized  $\Lambda$  and  $\bar{\Lambda}$  hyperons, aligned with the angular momentum of the colliding system. These measurements provide important information on partonic spin-orbit coupling, the vorticity of the quark-gluon plasma, and the magnetic field generated in the collision.

## 1. Introduction

Collisions of nuclei at ultra-relativistic energies create a system of deconfined colored quarks and gluons, called the quark-gluon plasma (QGP). The large angular momentum ( $\sim 10^4 - 5 \hbar$ ) present in non-central collisions may produce a polarized QGP, in which quarks are polarized through spin-orbit coupling in QCD [1, 2, 3]. The polarization would be transmitted to hadrons in the final state and could be detectable through global hyperon polarization.

Global hyperon polarization refers to the phenomenon in which the spin of  $\Lambda$  (and  $\bar{\Lambda}$ ) hyperons is correlated with the net angular momentum of the QGP which is perpendicular to the reaction plane, spanned by  $\vec{p}_{\text{beam}}$  and  $\vec{b}$ , where  $\vec{b}$  is the impact parameter vector of the collision and  $\vec{p}_{\text{beam}}$  is the beam momentum. This is distinct from the effect in  $p + p$  and  $p + A$  collisions, in which  $\Lambda$  are polarized relative to the production plane of the particle, spanned by  $\vec{p}_{\text{beam}}$  and  $\vec{p}_{\Lambda}$ . The latter effect is found in the beam fragmentation region (*i.e.* at forward rapidity) and vanishes by symmetry at midrapidity as well as for averages in azimuthal angle<sup>2</sup>. Global polarization, on the other hand, is expected for  $\Lambda$  and  $\bar{\Lambda}$  alike.

Global polarization has also been predicted in hydrodynamic calculations of non-central collisions [4, 5, 6]. Hydrodynamic approaches have been remarkably successful in describing the QGP and have allowed the

<sup>1</sup>A list of members of the STAR Collaboration and acknowledgements can be found at the end of this issue.

<sup>2</sup>In principle, convolution of the production-plane polarization with finite directed flow may produce a global effect. We estimate this to be far smaller than the signals we report here, in agreement with other estimates [4].

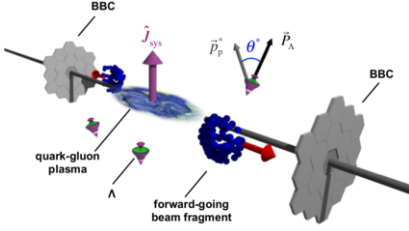


Fig. 1. The polarization,  $\vec{P}_\Lambda$ , of hyperons (drawn as spinning tops), drives the distribution of daughter proton momentum in the  $\Lambda$  rest frame,  $\vec{p}_p^*$ .

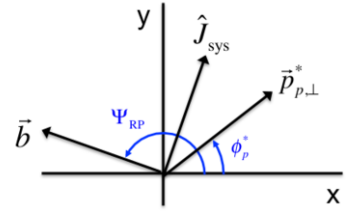


Fig. 2. The angles used in equation 2 are shown; here,  $\vec{p}_{p,\perp}^*$  is the component of the daughter proton's momentum transverse to the beam, in the  $\Lambda$  rest frame.

extraction of transport coefficients, including an exceptionally low shear viscosity. The vorticity is sensitive to the initial conditions [4, 5, 6], as well as the viscosity [5, 6] and temperature [7] of the fluid as it evolves. A vortical structure of the velocity field has also been recently reported in microscopic transport simulations of heavy-ion collisions at RHIC [8].

Hyperon polarization may also arise due to a coupling of the hadronic magnetic dipole moment  $\vec{\mu}_H$  to the magnetic field  $\vec{B}$  produced in a non-central heavy-ion collision. Whereas the spin-orbit and vortical effects will generate a positive polarization for both  $\Lambda$  and  $\bar{\Lambda}$ , the magnetic coupling will generate a positive contribution for  $\bar{\Lambda}$  and a negative one for  $\Lambda$ . Effects related to the strong magnetic field produced in non-central heavy-ion collisions are currently the subject of intense study [9], and the splitting between  $\Lambda$  and  $\bar{\Lambda}$  polarization may provide a unique probe of the magnetic field.

## 2. Method and Results

We report the first observation of global hyperon polarization in heavy-ion collisions. The measurements were performed by the STAR experiment at RHIC, in Au+Au collisions at center-of-mass energies per nucleon pair of  $\sqrt{s_{NN}} = 7.7, 11.5, 14.5, 19.6, 27,$  and  $39$  GeV. About 130M minimum-bias events that pass standard quality cuts were recorded at  $\sqrt{s_{NN}} = 39$  GeV. The numbers of events were smaller at lower energies, with  $\sim 4$ M good minimum-bias events recorded at  $\sqrt{s_{NN}} = 7.7$  GeV. In this report, we focus on mid-central collisions, 20-50% of the total inelastic cross-section as estimated from the charged-particle yield at midrapidity measured in the STAR TPC.

The azimuthal angle of the impact parameter,  $\Psi_{RP}$ , is estimated by reconstructing the first-order event plane,  $\Psi_{EP}^{(1)}$ , in two Beam-Beam Counters (BBCs) covering the pseudorapidity range  $3.3 < |\eta| < 5.0$ . At the collision energies studied in this analysis, the directed flow of charged particles in this pseudorapidity region is positive at positive rapidities. Taking into account that the spectators “bounce-off” outward from the center of the system [10], this allows the determination of the angular momentum direction (Fig. 2). The event plane resolution,  $R_{EP}^{(1)} = \langle \cos(\Psi_{EP}^{(1)} - \Psi_{RP}) \rangle$ , is about 0.65 for mid-central events at  $\sqrt{s_{NN}} = 7.7$  GeV and decreases with energy to about 0.2 at  $\sqrt{s_{NN}} = 39$  GeV.

Hyperons were reconstructed in the TPC via the decay channel  $\Lambda \rightarrow p + \pi^-$  ( $\bar{\Lambda} \rightarrow \bar{p} + \pi^+$ ). The charged daughters were identified through their specific energy loss in the gas of the TPC for  $|\vec{p}| \lesssim 0.6$  GeV/c, and with the Time of Flight (TOF) detector for momenta up to 2.5 GeV/c. Hyperon candidates are identified according to topological properties of the decay vertex. The availability of TOF information for the daughter tracks was used as a proxy for track quality and the cuts used are quoted (in cm) for the cases of (both tracks are TOF matched, only the proton is matched, neither track is matched) – the case where only the pion is matched is poorly populated and was not used due to concerns about how these candidates added a systematic sensitivity of the analysis to the cut choices. The properties used for identification are the apparent decay length of the hyperon (2, 2.5, 4) as well as the projected distance of closest approach (DCA) of the proton to the primary vertex (0.1, 0.15, 0.6), that of the pion to the primary vertex (0.7, 0.8, 1.7), of the parent hyperon to the primary vertex (1.3, 1.2, 0.75), and of the daughters to each other (1, 1, 1).

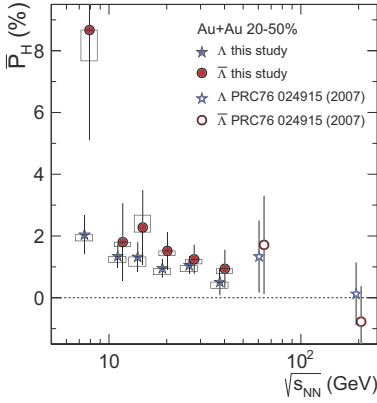


Fig. 3. The average polarization  $\bar{P}_H$  from 20-50% central Au+Au collisions is plotted as a function of collision energy. The results of the present study ( $\sqrt{s_{NN}} < 40$  GeV) are shown together with those reported earlier [11] for 62.4 and 200 GeV collisions, for which only statistical errors are plotted. The effects of feed-down have not been removed. Boxes indicate the systematic errors. See text for a discussion.

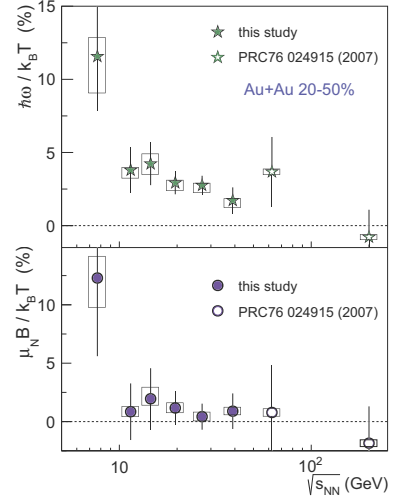


Fig. 4. The vorticity (top panel) and magnetic field (bottom) extracted from the polarization as shown in Fig. 3.

We focus on  $\Lambda$  and  $\bar{\Lambda}$  hyperons because their decay topology reveals their polarization. In the  $\Lambda$  ( $\bar{\Lambda}$ ) rest frame, the daughter proton (antiproton) tends to be emitted along (opposite) the parent's polarization direction. If  $\theta^*$  is the angle between the daughter proton (antiproton) momentum and the hyperon polarization vector  $\vec{P}_H$  in its rest frame (see Fig. 2), then

$$\frac{dN}{d \cos \theta^*} = \frac{1}{2} \left( 1 + \alpha_H |\vec{P}_H| \cos \theta^* \right). \quad (1)$$

The subscript H denotes  $\Lambda$  or  $\bar{\Lambda}$ ;  $\alpha_\Lambda = 0.642$  and  $\alpha_{\bar{\Lambda}} = -0.642$ .

Symmetry demands that, averaged over all phase space,  $\vec{P}_H$  is parallel to  $\hat{J}_{\text{sys}}$ , the unit vector in the direction of the angular momentum of the system. Both the magnitude ( $0 \leq |\vec{P}| \leq 1$ ) and direction of  $\vec{P}$  may depend strongly on transverse momentum, azimuthal angle and rapidity. The limited statistics of the datasets prohibit extensive exploration of these dependences, and we extract only the average projection of the polarization on  $\hat{J}_{\text{sys}}$ . It may be shown [11] that

$$\bar{P}_H \equiv \langle \vec{P}_H \cdot \hat{J}_{\text{sys}} \rangle = \frac{8}{\pi \alpha_H} \frac{\langle \sin(\phi_p^* - \Psi_{\text{EP}}^{(1)}) \rangle}{R_{\text{EP}}^{(1)}}, \quad (2)$$

where  $\Psi_{\text{EP}}^{(1)}$  is the angle of the first-order event plane that estimates the reaction plane angle  $\Psi_{\text{RP}}$ ,  $\phi_p^*$  is the azimuthal angle of the daughter proton (antiproton) in the hyperon rest frame. The overline on  $\langle \dots \rangle$  denote an average over the azimuthal angle of the hyperon momentum. Since  $R_{\text{EP}}^{(1)}$  depends on the collision centrality, in the present analysis we calculate  $\bar{P}_H$  separately for events of centrality 20-30%, 30-40%, and 40-50%, and report the weighted (with particle yield) average.

The results are shown in Fig. 3. At collision energies below 39 GeV, a significant polarization is observed for both  $\Lambda$  and  $\bar{\Lambda}$ , at the level of 1.5-3.5 times the statistical uncertainty. While including a broader centrality range into the analysis increases the hyperon statistics, the significantly poorer event plane resolution for more central or more peripheral collisions reduces the significance of the signal.

The results in Fig. 3 have been corrected for the dilution of the signal due to the combinatoric background of  $p + \pi$  pairs that pass our topological criteria and fall within the selected invariant mass window; this corresponds to a  $\sim 55\%$  ( $\sim 35\%$ ) correction for  $\Lambda$  ( $\bar{\Lambda}$ ) for most data points. A very small residual signal, at the level of the statistical uncertainty, is observed in the combinatoric background for  $p - \pi$  pairs with invariant mass slightly different from the  $m_\Lambda$ . The event sample sizes do not allow a full study of this residual correlation. Including this residual correlation in the combinatoric background correction leads to a downward shift of the order of 0.2% for most data points; this effect is indicated as a systematic uncertainty represented as asymmetric errors in Fig. 3; once again, the effect is somewhat larger for the  $\sqrt{s_{NN}} = 14.5$  GeV data.

Systematic errors associated with reasonable variation of topological cuts to select  $\Lambda$  candidates are negligible when compared to the statistical errors. The systematic error associated with the uncertainty in the event-plane resolution is  $\sim 2\%$ , much smaller than the statistical errors. The detector acceptance effects (due to hyperon reconstruction efficiency dependence on decay topology) [11] are  $\sim 3\%$ .

Both  $\Lambda$  and  $\bar{\Lambda}$  exhibit a similar and positive polarization, consistent with a common spin-orbit or vortical origin. While the difference is on the order of the uncertainties,  $\bar{P}_{\bar{\Lambda}}$  is slightly larger than  $\bar{P}_\Lambda$  at all collision energies, suggesting the possibility of an additional magnetic contribution. This difference could also arise due to the finite baryonic chemical potential [12].

The fluid vorticity may be estimated from the data using the hydrodynamic relation [13],

$$\omega \approx k_B T (\bar{P}_{\Lambda'} + \bar{P}_{\bar{\Lambda}'}) / \hbar, \quad (3)$$

where  $T$  is the temperature of the fluid at the moment when particles are emitted from it. The subscripts ( $\Lambda'$  and  $\bar{\Lambda}'$ ) in equation 3 indicate that these polarizations are for “primary” hyperons emitted directly from the fluid. However, most of the  $\Lambda$  and  $\bar{\Lambda}$  hyperons at these collision energies are not primary, but are decay products from heavier particles (e.g.  $\Sigma^{*,+} \rightarrow \Lambda + \pi^+$ ), which themselves would be polarized by the fluid. The data in Fig. 3 contain both primary and these “feed-down” contributions. At these collision energies, the effect of feed-down is estimated [13] to produce only  $\sim 20\%$  differences between the polarization of “primary” and “all” hyperons. Using these estimates of the feed-down we arrive at the vorticity and magnetic fields depicted in Fig. 4. We see a clear vortical signal and a hint at a magnetic field signal.

### 3. Conclusions

We have reported the first observation of global  $\Lambda$  and  $\bar{\Lambda}$  polarization in mid-central (20-50%) heavy-ion collisions. The signal is of the order of a few percent and falls with increasing collision energy. Theoretical calculations [3, 4, 7] for collisions at  $\sqrt{s_{NN}} = 200$  GeV predict  $\bar{P}_H \approx 0.5 - 2\%$ , and others suggest [5, 8] that the signal may be larger at lower  $\sqrt{s_{NN}}$ . The discovery of global hyperon polarization in heavy-ion collisions represents the first experimental evidence of the vortical structure of the quark gluon plasma, and provides constraints on magnetic effects in noncentral collisions. Further research on both the experimental and theoretical fronts is clearly required to understand these effects fully.

### References

- [1] Z.-T. Liang and X.-N. Wang, Phys. Rev. Lett. **94**, 102301 (2005) [Erratum: Phys. Rev. Lett. **96**, 039901 (2006)]
- [2] S. A. Voloshin, arXiv:0410089
- [3] J.-H. Gao, S.-W. Chen, W. Deng, Z.-T. Liang, Q. Wang, and X.-N. Wang, Phys. Rev. C **77**, 044902 (2008)
- [4] F. Becattini, L. Csernai, and D. J. Wang, Phys. Rev. C **88** (3), 034905 (2013)
- [5] B. Betz, M. Gyulassy, and G. Torrieri, Phys. Rev. C **76**, 044901 (2007)
- [6] F. Becattini, G. Inghirami, V. Rolando, A. Beraudo, L. Del Zanna, A. De Pace, M. Nardi, G. Pagliara, and V. Chandra, Eur. Phys. J. C **75** (9), 406 (2015)
- [7] L. P. Csernai, F. Becattini, and D. J. Wang, J. Phys. Conf. Ser. **509**, 012054 (2014)
- [8] Y. Jiang, Z.-W. Lin, and J. Liao, arXiv:1602.06580
- [9] D. E. Kharzeev, J. Liao, S. A. Voloshin, and G. Wang, Prog. Part. Nucl. Phys. **88**, 128 (2016)
- [10] S. A. Voloshin and T. Niida, arXiv:1604.04597
- [11] STAR Collaboration, Phys. Rev. C **76**, 024915 (2007)
- [12] F. Becattini, V. Chandra, L. Del Zanna, and E. Grossi, Annals Phys. **338**, 3249 (2013)
- [13] F. Becattini, I. Karpenko, M. Lisa, I. Upsal, and S. Voloshin, Phys. Rev. C **95**, 054902 (2017)